Original articles

Structure and electrical transport properties of cation-deficient derivatives of layered neodymium–barium ferrocuprocobaltite

E. A. Chizhova, M. V. Marozau, S. V. Shevchenko, A. I. Klyndyuk✉, Ya. Yu. Zhuravleva, V. M. Kononovich

*Belarusian State Technological University,
13A Sverdlova str., Minsk 220006, Republic of Belarus*

Abstract

Layered double perovskites (LDP) based on rare earth elements, barium, and 3d-metals with high electrical conductivity and electrocatalytic activity in the oxygen reduction reaction are promising cathode materials for medium-temperature solid oxide fuel cells based on proton- or oxygen-conducting solid electrolytes. For the improvement of the functional characteristics of LDP, various strategies are used: a) creating composites based on LDP, b) the partial substitution of cations, and c) the creation of a deficiency of cations in various positions in the LDP structure. The advantage of the latter strategy is that it does not require complicating the chemical and, as a rule, phase composition of the LDP. The purpose of this study was the investigation of the effect of neodymium and barium deficiency on the structural and electrical transport characteristics of $NdBaFeCo_{0.5}Cu_{0.5}O_{6-\delta}$ LDP.

The samples were obtained by the ceramic method and characterized using X-ray phase analysis, IR absorption spectroscopy, iodometry, electron microscopy, thermal analysis, as well as electrical conductivity and thermo-EMF measurements methods.

Creation of up to 10 mol. % of vacancies in neodymium or barium sublattices had little effect on the values of the oxygen nonstoichiometry index (δ) and unit cell parameters of $NdBaFeCo_{0.5}Cu_{0.5}O_{6-\delta}$ derivatives. However, it led to an increase in the crystallite size (determined by the Scherrer, Williamson–Hall and size–strain methods) and the thermal stability of these phases. The values of electrical conductivity and the Seebeck coefficient of ceramics, in general, increased, and the activation energies of the electrical transfer process decreased when a deficiency of neodymium or barium was created in its structure. In the temperature range 300–700 K, the weighted mobility of charge carriers ("holes") varied within 0.04–0.8 cm²/(V·s) and increased with increasing temperature, which is typical for the polaron conduction mechanism, and their concentration varied in the range $(0.1-3)\cdot10^{20}$ cm⁻³, increased exponentially with increasing temperature and, in general, when a deficiency of neodymium or barium in the $NdBaFeCo_{0.5}Cu_{0.5}O_{6-\delta}$ structure was created.

Keywords: Layered double perovskites, Cation deficiency, Structure, Thermal stability, Electrical conductivity, Thermo-EMF, Weighted mobility, Concentration of charge carriers

✉ Andrei I. Klyndyuk, e-mail: klyndyuk@belstu.by

1. Introduction

High values of electrical conductivity and the Seebeck coefficient of $LnBa(M',M'',M''')_2O_{6-\delta}$ (Ln– Y, rare earth element (REE), $M',M'',M''' - 3d$-metal) compounds, related to oxygen-deficient layered double perovskites (LDP), as well as the presence in their structure of electrochemically active transition metal ions and weakly bound oxygen determines the interest in these complex oxides as functional materials for various purposes, including high-temperature thermoelectrics, cathode materials of solid oxide fuel cells (SOFC), working elements of chemical semiconducting gas sensors, membranes for oxygen separation, etc. [1–4]. LDP are semiconductors with a band gap of about 1.5 eV [5].

Functional characteristics of $LnBa(M',M'',M''')_2O_{6-\delta}$ phases can be improved by introducing of nano- and microparticles of a different nature into them, the targeted substitution of cations, or creating their deficiency in various positions of the crystal structure of these compounds [3, 6–8], and the latter method of modification is interesting since it can be carried out without complication of the chemical composition of complex $LnBa(M',M'',M''')_2O_{6-\delta}$ oxides [9].

The authors [10–12] found that cation-deficient $Ln_{1-x}BaCo_2O_{6-\delta}$ (Ln – Pr, Nd, Sm) LDP were formed when the deficiency of cations in the REE sublattice of their structure up to 5 mol. % was created. A deficiency of REE in LDP promoted the formation of oxygen vacancies in their structure, which led to an increase in the parameters of the crystal structure and a slight decrease in electrical conductivity [10–12]. However, it significantly reduced their specific surface resistance and increased the output power of electrochemical cells in which they act as cathodes [11].

The creation of barium deficiency in the structure of layered cobaltites $LnBaCo_2O_{6-\delta}$ (Ln – La, Pr, Nd, Sm) [10, 13–19], in general, similarly affected the oxygen nonstoichiometry, structural characteristics, electrical transport properties, and electrochemical performance of these phases, although several differences were observed. Thus, the width of the barium homogeneity region of the $LnBaCo_2O_{6-\delta}$ phases was wider than for REE, and reaches 10 and 15 mol. % for Ln = Pr [15,

16] and Ln = La [13], respectively. Parameters of the unit cell of $LnBa_{1-x}Co_2O_{6-\delta}$ (Ln – Pr, Nd) LDP decreases slightly, and the electrical conductivity of ceramics increases significantly when a barium deficiency is created in it [15–17], while the greatest increase in electrical conductivity was observed for $PrBa_{0.92}Co_2O_{6-\delta}$ [14], $PrBa_{0.96}Co_2O_{6-\delta}$ [15], $NdBa_{0.95}Co_2O_{6-\delta}$ [17] samples.

It was established in [20] that the creation of cobalt deficiency in the structure of the complex oxide $PrBaCo_2O_{6-\delta}$ led to an increase in unit cell parameters, oxygen nonstoichiometry index, and a decrease in electrical conductivity and specific surface resistance of $PrBaCo_{2-x}O_{6-\delta}$ phases and an increase in the output power of cells in which they acted as cathodes, and a composition with $x = 0.06$ was characterized by the highest electrochemical performance.

Layered $LnBaCo_2O_{6-\delta}$ cobaltites had the highest electrochemical activity in the oxygen reduction reaction among LDP, however, their thermal expansion coefficients (TEC) significantly exceeded those for typical solid electrolytes (SE) [2–4,7,8]. In this regard, a low thermomechanical compatibility of SE and $LnBaCo_2O_{6-\delta}$ was observed, which limited the practical use of REE–barium cobaltites in various SOFC. A decrease in the TEC of layered cobaltites can be caused by the partial substitution of cobalt in their structure with other $3d$-metals, which in many cases also led to an improvement in the electrochemical performance of these phases [3]. Thus, the complex modification of layered $LnBaCo_2O_{6-\delta}$ oxides by partial substitution of cobalt in them and the creation of a deficiency of rare earth elements and barium can be considered as a promising method for developing electrode materials for medium-temperature SOFC with improved functional characteristics [18].

Previously, we studied the effect of cation deficiency in various sublattices of the $LnBaCuFeO_{6-\delta}$ (Ln – Y, La) structure on their oxygen stoichiometry $(6-\delta)$, crystal lattice parameters, thermal and electrical properties [21, 22], and it has also been shown that $NdBa(Fe,Co,Cu)O_{6-\delta}$ LDP are of interest as cathode materials for medium-temperature SOFC [23]. It was shown in [24] that the substitution of barium ions with strontium ions in $NdBaFeCo_{0.5}Cu_{0.5}O_{6-\delta}$ led to a decrease in

Condensed Matter and Interphases / Конденсированные среды и межфазные границы   2024;26(2): 339–348

E. A. Chizhova et al.   Structure and electrical transport properties of cation-deficient derivatives...

TEC and an increase in the electrical conductivity of this complex oxide.

The purpose of this study was investigation of the effect of neodymium and barium deficiency on the thermal stability and the structural and electrical transport characteristics of $NdBaFeCo_{0.5}Cu_{0.5}O_{6-\delta}$ LDP.

2. Experimental

LDP samples with the composition $Nd_{0.90}BaFeCo_{0.5}Cu_{0.5}O_{6-\delta}$ (N090B), $Nd_{0.95}BaFeCo_{0.5}Cu_{0.5}O_{6-\delta}$ (N095B), $NdBaFeCo_{0.5}Cu_{0.5}O_{6-\delta}$ (NB), $NdBa_{0.95}FeCo_{0.5}Cu_{0.5}O_{6-\delta}$ (NB095) and $NdBa_{0.90}FeCo_{0.5}Cu_{0.5}O_{6-\delta}$ (NB090) were synthesized using a standard ceramic method from neodymium (NO-L), iron (III) (extra pure grade 2–4), cobalt (II, III) (pure grade), and copper (II) (pure grade) oxides and barium carbonate (pure grade), which were mixed in specified stoichiometric ratios and grounded using a Pulverizette 6.0 mill from Fritsch (crucible material and grinding balls was ZrO_2). Then, the resulting powders were pressed into tablets with a diameter of 19 mm and a height of 2–3 mm, which were annealed in air for 40 h at 1173 K [23, 24]. Annealed samples were crushed in an agate mortar, re-grounded using a Pulverizette 6.0 mill (Fritsch) and pressed into bars with the size of 5×5×30 mm. The samples were sintered in air for 9 h at 1273 K. For the measurements of electrical conductivity, rectangular parallelepipeds with a size of 4×4×2 mm were cut from sintered ceramics.

The identification of samples and determination of their unit cell parameters were carried out using X-ray phase analysis (XRD) (X-ray diffractometer Bruker D8 XRD Advance, CuK_α-radiation) and IR absorption spectroscopy (Nexus ThermoNicolet IR Fourier spectrometer) ($\Delta\nu = \pm2$ cm^{-1}). The oxygen nonstoichiometry index of the samples (δ) were determined using iodometric titration according to the method [25] ($\Delta\delta = \pm0.01$), taking into account the presence of $3d$- metals in various oxidation states ($Fe^{+3}, Co^{+4}, Co^{+3}, Cu^{+2}$), which were reduced into Co^{+2}, Cu^+, and Fe^{+2} during titration.

The average size of coherent scattering areas (CSA, D), comparable to the crystallite sizes, were calculated based on the XRD results using the Scherrer equation (1) [26]:

$$D = \frac{K\lambda}{\beta\cos\Theta}, \tag{1}$$

where $K = 0.9$; λ – wavelength of CuK_α – radiation, nm; β – the width of the integral peak at half-maximum, rad; Θ – Bragg angle, rad.

Additionally, the CSA and microstrain values were calculated using the Williamson–Hall method (2) and the size–strain method (3) [27]:

$$\beta\cos\Theta = \frac{K\lambda}{D} + 4\varepsilon\sin\Theta, \tag{2}$$

$$\left(d\beta\cos\Theta\right)^2 = \frac{K\lambda}{D}\left(d^2\beta\cos\Theta\right) + \left(\frac{\varepsilon}{2}\right)^2, \tag{3}$$

where ε – microstrain value; d – interplanar distance, nm.

Apparent density (ρ_{app}) ceramics were determined based on the geometric dimensions and the weight of the samples, the relative density (ρ_{rel}) of ceramics and its total porosity (Π) was calculated as:

$$\rho_{rel} = \frac{\rho_{app}}{\rho_{XRD}} \cdot 100\%, \tag{4}$$

$$\Pi = \left(\frac{\rho_{XRD} - \rho_{app}}{\rho_{XRD}}\right) \cdot 100\%, \tag{5}$$

where ρ_{XRD} – theoretical (X-ray) density of samples.

Open porosity (Π_o) was determined based on the water absorption of the samples, and closed (Π_c) porosity was determined as the difference between total and open porosity.

The microstructure of the samples was studied by scanning electron microscopy (SEM) using JSM-5610 LV scanning electron microscope, as well as using an ALTAMI MET 1D digital metallographic microscope (Altami, Russian Federation).

The thermal stability of LDP powders was studied in air in the temperature range 300–1100 K using a TGA/DSC–1/1600 HF thermoanalytical system. Electrical conductivity (σ) and thermo-EMF (S) of the resulting ceramic samples, after applying contacts to their ends by burning silver paste, were studied in air in the temperature range of 300–1100 K according to the methods of [21, 22] ($\delta\sigma \leqslant 5$ %, $\delta S \leqslant 10$ %). Conduction (E_σ) and thermo-EMF activation energies of samples

(E_S) were calculated from the linear parts of the dependences $\ln(\sigma \cdot T) = f(1/T)$ and $S = f(1/T)$, respectively. Weighted mobility of the main charge carriers (μ), as well as their concentration (p) were calculated based on experimentally determined values of electrical conductivity (σ) and Seebeck coefficient (S) of cation-deficient ceramics using the method [28]. The activation energy of the main charge carriers (E_p) was calculated based on the dependences $\ln p = f(1/T)$, using the equation:

$$p = p_0 \exp\left[-\frac{E_p}{kT}\right], \tag{6}$$

where p_0 – constant, k – Boltzmann constant, T – temperature.

3. Results and discussion

After the final stage of synthesis, all samples, within the error of X-ray phase analysis, were single-phase (Fig. 1a) and had a double perovskite structure ($a = b \approx a_p$, $c \approx 2a_p$, sp. gr.$P4/mmm$ [18, 23]). The crystal lattice parameters of the cation-deficient samples were close to those for the base phase (NB) (Table 1) and increased slightly when vacancies were created in the neodymium sublattice, which is consistent with the results of [10–12]. The axial ratio ($c/2a$) of the samples, in general, increased with the formation of neodymium or barium vacancies in their structure, which indicates a decrease in the degree of tetragonal distortion of their perovskite structure.

The value of the oxygen nonstoichiometry index of the double perovskites obtained in this study varied within the range of 0.28–0.32 (Table 1), slightly increasing when a deficiency of cations in the structure of the NdBaFeCo$_{0.5}$Cu$_{0.5}$O$_{6-\delta}$ phase was created.

In the IR absorption spectra of the studied LDP samples (Fig. 1b), four expressed absorption bands with extrema at 357–374 cm^{-1} (ν_1), 467–468 cm^{-1} (ν_2), 577–580 cm^{-1} (ν_3) and 650–661 cm^{-1}
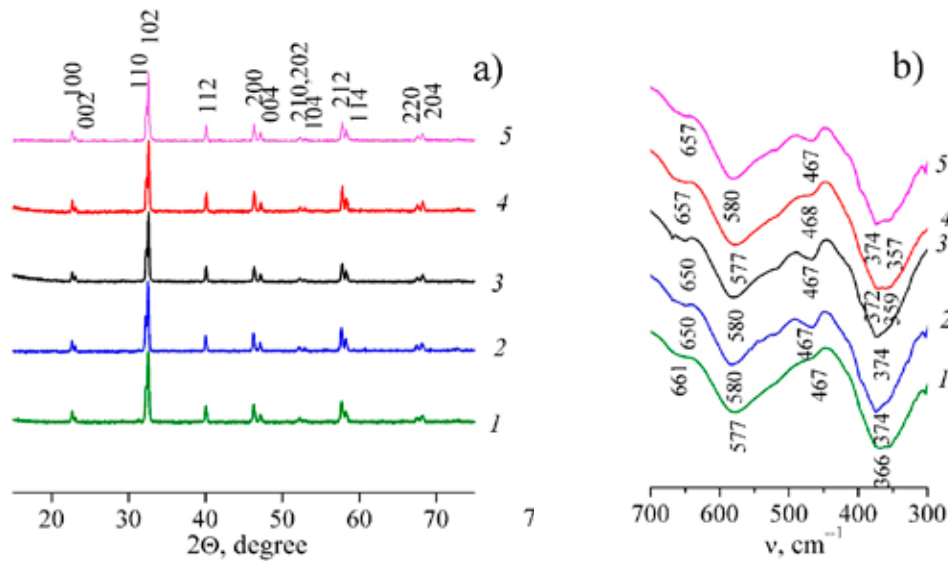
Fig. 1. X-ray powder diffractogramms (a) and IR absorption spectra (b) of N090B (*1*), N095B (*2*), NB (*3*), NB095 (*4*), NB090 (*5*)

Table 1. Lattice constants (*a*, *c*, *V*), tetragonal distortion degree (*c/2a*) and oxygen nonstoichiomety index of cation-deficient NdBaFeCo$_{0.5}$Cu$_{0.5}$O$_{6-\delta}$ perovskites

Sample	*a*, nm	*c*, nm	*V*, nm³	*c/2a*	δ
N090B	0.39274	0.77267	0.1192	0.9837	0.30
N095B	0.39261	0.77095	0.1188	0.9818	0.32
NB	0.39212	0.77072	0.1185	0.9828	0.28
NB095	0.39145	0.76965	0.1179	0.9831	0.30
NB090	0.39182	0.77128	0.1184	0.9842	0.31

Condensed Matter and Interphases / Конденсированные среды и межфазные границы   2024;26(2): 339–348

E. A. Chizhova et al.   Structure and electrical transport properties of cation-deficient derivatives...

(v_4) were observed, which according to [29] correspond to valence (v_2, v_3) and deformation vibrations of bonds (Fe,Co,Cu)–O–(Fe,Co,Cu) in layers [(Fe,Co,Cu)O_2] (v_1–v_3) of crystal structure of these phases and in the direction perpendicular to these layers (v_4), and for compositions NB095 and NB090, splitting of v_1 band into two with extremes at 357–359 and 372–374 cm^{-1} was noted. The position of the extrema in the IR absorption spectra of the samples practically did not change with changes in their cation composition, which was in good agreement with the results of X-ray diffraction and iodometry, according to which the creation of a deficiency of cations in the structure of NdBaFeCo$_{0.5}$Cu$_{0.5}$O$_{6-\delta}$ LDP has little effect on the parameters of its crystal structure and oxygen stoichiometry.

The CSA values corresponding to the average crystallite sizes in the samples, determined by various methods, were somewhat different from each other (Table 2, Fig. 2), however, there was a pronounced tendency towards an increase in the CSA with an increase in the cation deficiency in the LDP structure, explained by an increase in the diffusion mobility of the elements of their crystal structure with an increase in the degree of its defectness. The microstrain values of the samples determined using the Williamson–Hall and size–strain methods were close, with the exception of the N090B composition, characterized by significantly higher values ε. According to the results of microscopy, the ceramic grains had a shape close to isometric, and their size was 3–5 μm and practically did not change with changes in the cationic composition of the ceramic. Thus, the grains of the studied ceramics turned out to be polycrystalline and contained several tens crystallites each.

The apparent density of ceramics increased, and its porosity, accordingly, decreased with increasing deficiency of neodymium or barium cations in its composition (Table 3). This finding indicates that the sintering of ceramics based on the NdBaFeCo$_{0.5}$Cu$_{0.5}$O$_{6-\delta}$ phase increased with
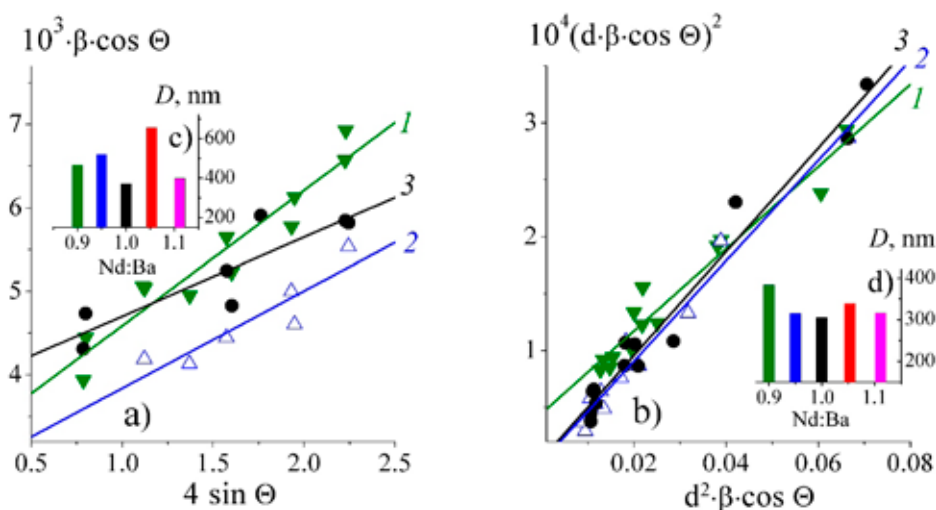
Fig. 2. Williamson–Hall (a) and size–strain plots (b) of N090B (*1*), N095B (*2*), NB (*3*), coherent scattering area values (c, d)

Table 2. Values of coherent scattering area (*D*) and microstrains of NdBaFeCo$_{0.5}$Cu$_{0.5}$O$_{6-\delta}$ ceramic samples, calculated using Sherrer, Williamson–Hall, and size–strain (S–S) methods

Sample	Sherrer	Williamson–Hall		S–S	
	D, nm	*D*, nm	ε	*D*, nm	ε
N090B	252.9	467.4	0.0016	384.6	0.0134
N095B	303.8	519.9	0.0012	314.8	0.0033
NB	288.7	370.2	0.0009	305.1	0.0044
NB095	330.8	655.0	0.0010	339.4	0.0029
NB090	293.2	398.9	0.0008	316.2	0.0024

Condensed Matter and Interphases / Конденсированные среды и межфазные границы   2024;26(2): 339–348

E. A. Chizhova et al.   Structure and electrical transport properties of cation-deficient derivatives...

Table 3. X-ray (ρ_{XRD}), apparent (ρ_{app}), relative (ρ_{rel}) density, full (Π), open (Π_o), and closed (Π_c) porosity of $NdBaFeCo_{0.5}Cu_{0.5}O_{6-\delta}$ ceramics

Образец	ρ_{XRD}, g/cm³	ρ_{app}, g/cm³	ρ_{rel}, %	Π, %	Π_o, %	Π_c, %
N090B	6.47	6.08	94.0	6.0	1.9	4.1
N095B	6.59	6.09	92.4	7.6	2.3	5.3
NB	6.71	6.06	90.3	9.7	5.7	4.0
NB095	6.65	6.39	96.1	3.9	1.7	2.2
NB090	6.52	6.17	94.6	5.4	1.8	3.6

the creation of cation vacancies in its structure, which, as mentioned above, is explained by an increase in the diffusion mobility of the cations included in their composition due to an increase in the defectiveness of the crystal structure of LDP. The highest value of apparent density (6.39 g/cm³) and the lowest porosity (3.9%) were recorded for composition NB095. It is interesting to note that the creation of cation vacancies predominantly reduced the open porosity of the ceramics, while the closed porosity of the cation-deficient samples varied within a fairly narrow range (3.6–5.3%) and was close to that for the base composition (NB) (4.0%), with the exception of the NB095 sample, characterized by the lowest closed porosity (2.2%) (Table 3).

Based on the results of thermal analysis (Fig. 3), we can conclude that the studied powders were thermally stable up to temperatures T^* = 685–745 K, above which some (≈0.3–0.5%)

weight loss caused by the release of mobile oxygen from samples ($1-\delta$) and an increase in the oxygen nonstoichiometry index (Fig. 3b) were observed [23–25]. In this case, the highest weight loss was observed for the composition N090B, and the lowest for samples N095B and NB090 (Fig. 3a). The T^* value was minimal for the basic $NdBaFeCo_{0.5}Cu_{0.5}O_{6-\delta}$ LDP and increased when a deficiency of neodymium or barium was created in its structure (Fig. 3c). Thus, the creation of vacancies in the sublattices of neodymium or barium of the $NdBaFeCo_{0.5}Cu_{0.5}O_{6-\delta}$ phase led to an increase in its thermal stability. It should be noted that the thermal stability and sintering ability of the studied samples, in general, change symbatically with changes in their cation composition, which is in good agreement with the results we obtained earlier when studying LDP in the $NdBaFeCo_{0.5}Cu_{0.5}O_{6-\delta}$–$NdSrFeCo_{0.5}Cu_{0.5}O_{6-\delta}$ system [24].

The studied LDP are semiconductors ($\partial\sigma/\partial T > 0$) of p-type ($S > 0$) (Fig. 4a, b), the nature of the electrical conductivity of which changes to metallic ($\partial\sigma/\partial T < 0$) near T_{max} = 992–1050 K (Fig. 4d). In this case, a change in the nature of the temperature dependence of their Seebeck coefficient was observed (from $\partial S/\partial T < 0$ at $T < T_{min}$ = 900–1052 K (Fig. 4f) to $\partial S/\partial T > 0$ at $T > T_{min}$), which was due to the release of mobile oxygen from the ceramic structure ($1-\delta$). The T_{max} and T_{min} values were significantly higher T^* = 685–745 K (Fig. 3b), since the release of oxygen from the volume of sintered ceramics into the gas phase (air) occurs with greater diffusion difficulties than from powders. A comparison of the results of this study with the data we obtained earlier investigating the electrical transport properties of LDP [21–25] allowed us to conclude that the conductivity of ceramics is determined by the electrical conductivity of the

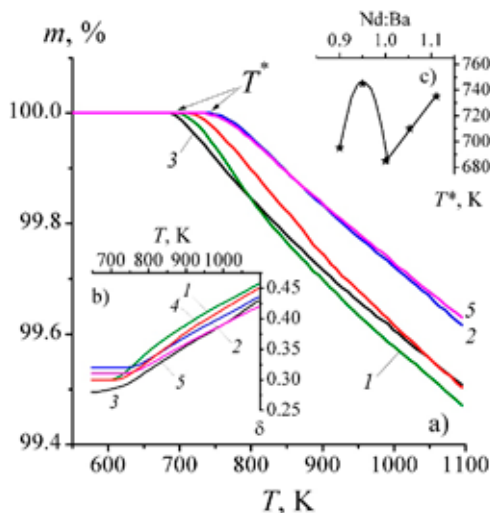**Fig. 3.** Depencences of mass loss (a), and oxygen non-stoihiometry index (b) of N090B (*1*), N095B (*2*), NB (*3*), NB095 (*4*), NB090 (*5*) phases vs temperature, and dependence of temperature of beginning of mass loss (c) of these compounds vs their composition

Condensed Matter and Interphases / Конденсированные среды и межфазные границы   2024;26(2): 339–348

E. A. Chizhova et al.   Structure and electrical transport properties of cation-deficient derivatives...
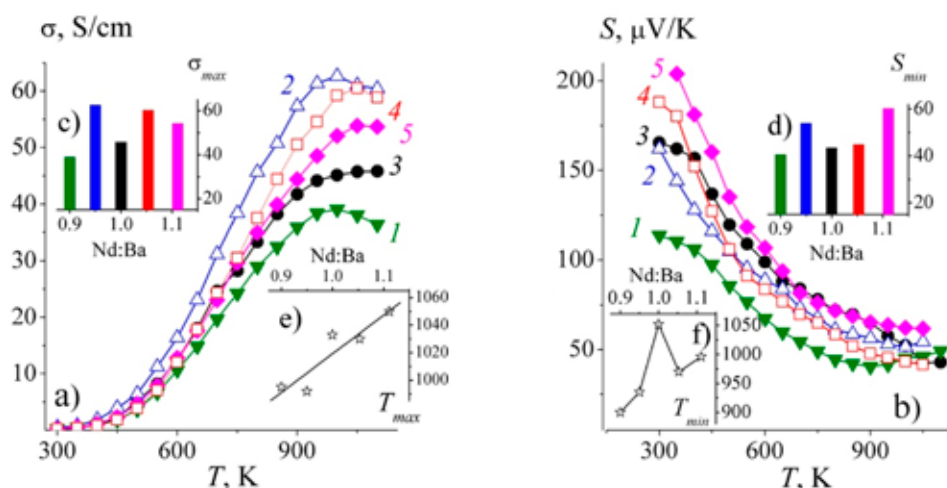
Fig. 4. Temperature (a, b) and concentration (c–f) dependences of electrical conductivity (a, c), Seebeck coefficient (b, d), and temperatures of extrema on the $\sigma = f(T)$ (e) and $S = f(T)$ (f) dependences of N090B (*1*), N095B (*2*), NB (*3*), NB095 (*4*), NB090 (*5*) ceramics

grains, the contributions of grain boundaries and contacts are insignificant, and the ohmicity of the contacts is confirmed by the linearity of their current-voltage characteristics. The values of the electrical conductivity and the Seebeck coefficient of ceramics, in general (with the exception of N090B composition), increase when a deficiency of cations is created in it (Fig. 4c, d, Table 4). The temperature T_{max} value on dependencies $\sigma = f(T)$ for the studied LDP, in general, increased with increasing Nd:Ba ratio in its structure, while the temperature T_{min} on dependencies $S = f(T)$ was maximal for the basic composition (NB) and decreased when neodymium or barium vacancies were created in its structure (Fig. 4e, f, Table 4).

The LDP investigated in this study were polaronic conductors [3, 10–17, 21–24], for which the dependence of electrical transport properties on temperature is described by the equations:

$$\sigma = \frac{A}{T}\exp\left[-\frac{E_\sigma}{kT}\right], \qquad (7)$$

$$S = \frac{k}{e}\left(-\frac{E_S}{kT} + B\right), \qquad (8)$$

where k – Boltzmann constant, T - temperature, A and B – constants, $E_\sigma = E_S + E_m$ and E_S – activation energies of electrical conductivity and thermo-EMF, E_S – the excitation energy of polarons, and E_m – activation energy of their transfer [30]. As can be seen from the data in Table 4, the activation energies of the electrical transfer process (E_σ, E_S and E_m) in the studied ceramic samples, in general, decreased when a deficiency of neodymium or barium was created. For the studied LDP $E_\sigma > E_S$ ($E_m > 0$) (Table 4), from which it follows that the charge carriers in them are small radius polarons (SRP).

Weighted mobility of charge carriers (μ) in the studied samples in the temperature range

Table 4. Values of electrical conductivity at room temperature (σ_{300}), maximal electrical conductivity (σ_{max}), minimal Seebeck coefficient (S_{min}), temperatures of extrema on the temperature dependences of electrical conductivity and Seebeck coefficient (T_{max}, T_{min}), and activation energies of electrical transport (E_σ, E_S, E_m) in the NdBaFeCo$_{0.5}$Cu$_{0.5}$O$_{6-\delta}$ ceramic samples

Sample	σ_{300}, S/cm	σ_{max}, S/cm	T_{max}, K	S_{min}, μV/K	T_{min}, K	E_σ, eV	E_S, eV	E_m, eV
N090B	0.230	39.1	995	40.6	900	0.281	0.051	0.230
N095B	0.461	62.6	992	53.9	935	0.267	0.049	0.218
NB	0.208	45.8	1033	43.5	1052	0.305	0.067	0.238
NB095	0.206	60.2	1030	44.8	970	0.308	0.069	0.239
NB090	0.250	54.2	1050	60.3	996	0.281	0.087	0.194

Condensed Matter and Interphases / Конденсированные среды и межфазные границы   2024;26(2): 339–348

E. A. Chizhova et al.   Structure and electrical transport properties of cation-deficient derivatives...

300–700 K varied within 0.04–0.8 cm²/(V·s) and increased with increasing temperature (Fig. 5a), which is characteristic for the polaron conduction mechanism. The values of μ changed non-monotonically with changes in the cation composition and oxygen nonstoichiometry index (δ) of samples (Fig. 5c, d). The concentration of charge carriers "holes" in the same temperature range varied within the range $(1-30)\cdot10^{19}$ cm^{-3} (Fig. 5b), in general, increased with the creation of a deficiency of neodymium or barium cations (Fig. 5e), as well as with increase in δ (Fig. 5e), and increased exponentially with increasing temperature. The activation energy of charge carriers (E_p), varied within 0.150–0.174 eV and increased with increasing Nd:Ba ratio in the structure of the ceramics.

4. Conclusions

Cation-deficient ceramics based on NdBaFeCo$_{0.5}$Cu$_{0.5}$O$_{6-\delta}$ LDP was obtained using solid-phase reactions. The structure, oxygen stoichiometry, thermal stability, electrical conductivity, and thermo-EMF of the samples were studied. It was shown that the creation of up to 10 mol. % deficiency of neodymium or barium in the NdBaFeCo$_{0.5}$Cu$_{0.5}$O$_{6-\delta}$ phase did not significantly affect the parameters of its crystal structure and oxygen nonstoichiometry index, but led to the growth of crystallites, improved the sintering of ceramics, increased its thermal stability, and improved the electrical transport properties. The activation energies of the processes of electrical transfer, weighted mobility and concentration of the main charge carriers ("holes") in the studied materials were calculated, the influence of the cationic composition and oxygen stoichiometry of ceramics on its structural, thermal and electrical transport characteristics were analyzed. The approach used in this study can be effectively applied to the development of electrode materials for medium-temperature solid oxide fuel cells based on oxygen-ion- or proton-conducting solid electrolytes.

Authors contributions

Chizhova E. A. – synthesis of materials, processing and interpreting the results, data visualization, writing the article. Marozau M. V. – conducting research, processing the results. Shevchenko S. V. – synthesis of materials, conducting research. Klyndyuk A. I. – scientific supervision, research concept, interpreting the results, final conclusions, writing the article. Zhuravleva Ya. Yu. – conducting research, processing and interpreting results. Kononovich V. M. - conducting research.

Conflict of interests

The authors declare that they have no known competing financial interests or personal relationships that could have influenced the work reported in this paper.

References

1. Jacobson A. J. Materials for solid oxide fuel cells. *Chemistry of Materials*. 2010;22(3): 660–670. https://doi.org/10.1021/cm902640j
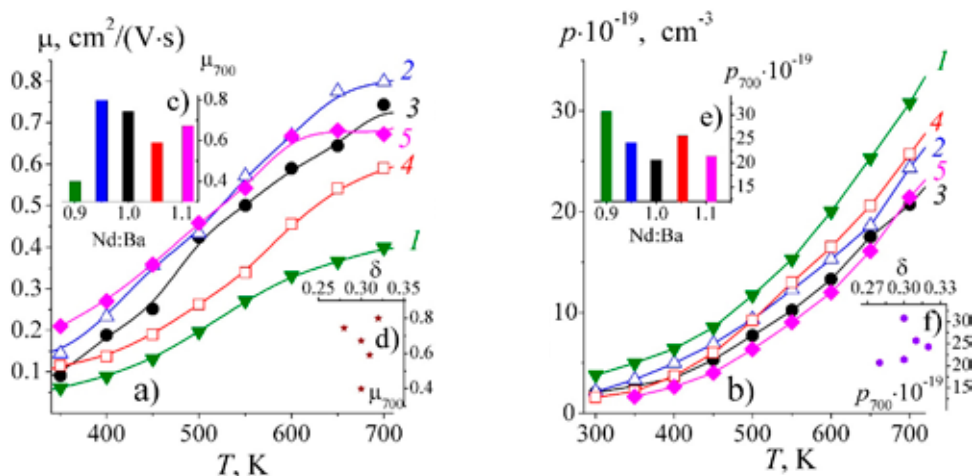

Fig. 5. Dependences of weighted mobility (a, c, e) and charge carriers concentration (b, d, f) in N090B (*1*), N095B (*2*), NB (*3*), NB095 (*4*), NB090 (*5*) ceramicsvs temperature (a, b) and composition of the samples (c–f)

Condensed Matter and Interphases / Конденсированные среды и межфазные границы   2024;26(2): 339–348

E. A. Chizhova et al.   Structure and electrical transport properties of cation-deficient derivatives...

2. Afroze S., Karim A. H., Cheok Q., Eriksson S., Azad A. K. Latest development of double perovskite electrode materials for solid oxide fuel cells: a review. *Frontiers in Energy*. 2019;13: 770–797. https://doi.org/10.1007/s11708-019-0651-x

3. Klyndyuk A. I., Chizhova E. A., Kharytonau D. S., Medvedev D. A. Layered oxygen-deficient double perovskites as promising cathode materials for solid oxide fuel cells. *Materials*. 2022;15(1): 141. https://doi.org/10.3390/ma15010141

4. Kumar R. M., Khandale A. P. A review on recent progress and selection of cobalt-based cathode materials for low temperature solid oxide fuel cells. *Renewable and Sustainable Energy Reviews*. 2022;156: 111985. https://doi.org/10.1016/j.rser.2021.111985

5. Zeng C., Zhan B., Butt S., … Nan C.–W. Electrical and thermal conduction behaviors in La-substituted $GdBaCuFeO_{5+\delta}$ ceramics. *Journal of American Ceramic Society*. 2015;98(10): 3179–3184. https://doi.org/10.1111/jace.13728

6. Tsvetkov D. S., Ivanov I. L., Malyshkin D. A., Sednev A. L., Sereda V. V., Zuev A. Yu. Double perovskites $REBaCo_{2-x}M_xO_{6-\delta}$ (RE = La, Pr, Nd, Eu, Gd, Y; M = Fe, Mn) as energy-related materials: an overview. *Pure and Applied Chemistry*. 2019;19(6): 923–940. https://doi.org/10.1515/pac-2018-1103

7. Kaur P., Singh K. Review of perovskite-structure related cathode materials for solid oxide fuel cells. *Ceramics International*. 2020;46: 5521–5535. https://doi.org/10.1016/j.ceramint.2019.11.066

8. Istomin S. Ya., Lyskov N. V., Mazo G. N., Antipov E. V. Electrode materials based on complex *d*-metal oxides for symmetrical solid oxide fuel cells. *Russian Chemical Reviews*. 2021;90(6): 644–676. https://doi.org/10.1070/RCR4979

9. Su Ch., Wang W., Shao Z. Cation-deficient perovskites for clean energy conversion. *Account of Materials Research*. 2021;2: 477–488. https://doi.org/10.1021/accountsmr.1c00036

10. Jiang X., Shi Y., Zhou W., … Jiang L. Effects of Pr^{3+}-deficiency on structure and properties of $PrBaCo_2O_{5+\delta}$ cathode material – A comparison with Ba^{2+}-deficiency case. *Journal of Power Sources*. 2014;272: 371–377. https://doi.org/10.1016/j.jpowsour.2014.08.091

11. Yi K., Sun L., Li Q., … Grenier J.-C. Effect of Nd-deficiency on electrochemical properties of $NdBaCo_2O_{6-\delta}$ cathode for intermediate-temperature solid oxide fuel cell. *International Journal of Hydrogen Energy*. 2016;41: 10228–10238. https://doi.org/10.1016/j.ijhydene.2016.04.248

12. Jiang X., Xu Q., Shi Y., … Zhang Q. Synthesis and properties of Sm^{3+}-deficient $Sm_{1-x}BaCo_2O_{5+\delta}$ perovskite oxides as cathode materials. *International Journal of Hydrogen Energy*. 2014;39: 10817–10823. http://dx.doi.org/10.1016/j.ijhydene.2014.04.203

13. Pang S. L., Jiang X. N., Li X. N., … Zhang Q. Y. Structure and properties of layered-perovskite $LaBa_{1-x}Co_2O_{5+\delta}$ (x = 0–0.15) as intermediate-temperature cathode material. *Journal of Power Sources*. 2013;240: 54–59. https://doi.org/10.1016/j.jpowsour.2013.04.005

14. Pang S., Jiang X., Li X., Wang Q., Su Z. Characterization of Ba-deficient $PrBa_{1-x}Co_2O_{5+\delta}$ as cathode material for intermediate temperature solid oxide fuel cells. *Journal of Power Sources*. 2012;204: 53–59. https://doi.org/10.1016/j.jpowsour.2012.01.034

15. Wang J., Meng F., Xia T., … Grenier J.-C. Superior electrochemical performance and oxygen reduction kinetics of layered perovskite $PrBa_xCo_2O_{5+\delta}$ (x = 0.90–1.00) oxides as cathode materials for intermediate-temperature solid oxide fuel cells. *International Journal of Hydrogen Energy*. 2014;39: 18392–18404. http://dx.doi.org/10.1016/j.ijhydene.2014.09.041

16. Pang S., Wang W., Chen T., … Fan J. The effect of potassium on the properties of $PrBa_{1-x}Co_2O_{5+\delta}$ (x = 0.00–0.10) cathodes for intermediate-tenperature solid oxide fuel cells. *International Journal of Hydrogen Energy*. 2016;41: 13705–13714. http://dx.doi.org/10.1016/j.ijhydene.2016.05.0460

17. Donazzi A., Pelosato R., Cordaro G., Stucchi D., Cristiani C., Dotelli G., Sora N. Evaluation of Ba deficient $NdBaCo_2O_{5+\delta}$ oxide as cathode material for IT-SOFC. *Electrochimica Acta*. 2015;182: 573–587. https://doi.org/10.1016/j.electacta.2015.09.117

18. Cordaro G., Donazzi A., Pelosato R., … Dotelli G. Structural and electrochemical characterization of $NdBa_{1-x}Co_{2-y}Fe_yO_{5+\delta}$ as cathode for intermediate temperature solid oxide fuel cells. *Journal of Electrochemical Society*. 2020;167: 024502. https://10.1149/1945-7111/ab628b

19. Kim C. G., Woo S. H., Song K. E., … Kim J. H. Enhanced electrochimical properties of non-stoichiometric layered perovskites, $Sm_{1-x}BaCo_2O_{5+\delta}$, for IT-SOFC cathodes. *Frontiers in Chemistry*. 2021;9: 633863. https://doi.org/10.3389/fchem.2021.633868

20. Zhang L., Li Sh., Sun L., Huo L., Zhao H. Co-deficient $PrBaCo_{2-x}O_{6-\delta}$ perovskites as cathode materials for intermediate-temperature solid oxide fuel cells: enhanced electrochemical performance and oxygen reduction kinetics. *International Journal of Hydrogen Energy*. 2018;43: 3761–3775. https://doi.org/10.1016/j.ijhydene.2018.01.018

21. Klyndyuk A. I., Chizhova E. A. Structure and electrical and transport properties of cation-deficient samples of perovskite ferrocuprates $RBaCuFeO_{5+\delta}$ (R = Y, La). *Physics of the Solid State*. 2008;50(4): 603–608. https://doi.org/10.1134/S1063783408040021

22. Klyndyuk A. I., Chizhova E. A. Effect of cation deficiency on the structure and properties of layered lanthanum barium ferrocuprate. *Russian Journal of*

Condensed Matter and Interphases / Конденсированные среды и межфазные границы 2024;26(2): 339–348

E. A. Chizhova et al. Structure and electrical transport properties of cation-deficient derivatives...

Inorganic Chemistry. 2008;53(4): 524–529. https://doi.org/10.1134/S0036023608040074

23. Klyndyuk A. I., Kharytonau D. S., Mosiałek M., …Zimowska M. Double substituted NdBa(Fe,Co,Cu)$_2$O$_{5+\delta}$ layered perovskites as cathode materials for intermediate-temperature solid oxide fuel cells – correlation between structure and electrochemical properties *Electrochimica Acta*. 2022;411: 140062 https://doi.org/10.1016/j.electacta.2022.140062

24. Klyndyuk A. I., Zhuravleva Ya. Yu., Gundilovich N. N., Chizhova E. A. Structural, thermal, and electrical properties of solid solutions in the NdBaFeCo$_{0.5}$Cu$_{0.5}$O$_{5+\delta}$–NdSrFeCo$_{0.5}$Cu$_{0.5}$O$_{5+\delta}$ system. *Inorganic Materials*. 2023;59(1): 86–92. https://doi.org/10.1134/S0020168523010089

25. Klyndyuk A. I., Zhuravleva Ya. Yu. Structure and physicochemical properties of NdBa$_{1-x}$Ca$_x$FeCo$_{0.5}$Cu$_{0.5}$O$_{5+\delta}$ solid solutions (0.00 ≤ x ≤ 0.40). *Russian Journal of Inorganic Chemistry*. 2022;67(12):2084–2089. https://doi.org/10.1134/S0036023622601404

26. Goryachko A. I., Ivanin S. N., Buz'ko V. Yu. Synthesis, microstructural and electromagnetic characteristics of cobalt-zinc ferrite. *Condensed Matter and Interphases*. 2020;22(4): 446–452. https://doi.org/10.17308/kcmf.2020.22/3115

27. Nikam C. U., Kadam S. R., Shotole R. S., …Kale G. H. Williamson–Hall and size strain plot based micro-structural analysis and evaluation of elastic properties of Dy^{3+} substituted Co–Zn nano-spinels. *Journal of Physics: Conference Series*. 2023;2426: 012029. https://doi.org/10.1088/1742-6596/2426/1/012029

28. Snyder G. J., Snyder A. H., Wood M., Gurunathan R., Snyder B. H., Niu C. Wighted mobility. *Advanced Materials*. 2020;35: 2001537. https://doi.org/10.1002/adma.202001537

29. Atanassova Y. K., Popov V. N., Bogachev G. G., … Pissas M. Raman- and infrared active phonons in YBaCuFeO$_5$: experimental and lattice dynamics. *Physical Review B*. 1993;47: 15201–15207. https://doi.org/10.1103/PhysRevB.47.15201

30. Mott N., Davis E. *Electronic processes in non-crystalline materials*. 2nded. New York, USA, Oxford: Oxford University Press; 1979. 590 p.

Information about the authors

Ekaterina A. Chizhova, Cand. Sci. (Chem.), Associate Professor, Associate Professor at the Department of Physical, Colloid and Analytical Chemistry, Belarusian State Technological University (Minsk, Republic of Belarus).

https://orcid.org/0000-0002-2793-5071

chizhova@belstu.by

Maksim V. Marozau, Student, Belarusian State Technological University (Minsk, Republic of Belarus).

https://orcid.org/0009-0000-0819-9681

wozmor@mail.ru

Svetlana V. Shevchenko, Cand. Sci. (Chem.), Associate Professor at the Department of Physical, Colloid and Analytical Chemistry, Belarusian State Technological University (Minsk, Republic of Belarus).

https://orcid.org/0009-0007-6950-9939

shevchenko@belstu.by

Andrei I. Klyndyuk, Cand. Sci. (Chem.), Associate Professor, Associate Professor at the Department of Physical, Colloid and Analytical Chemistry, Belarusian State Technological University (Minsk, Republic of Belarus).

https://orcid.org/0000-0003-0566-4386

klyndyuk@belstu.by

Yana Yu. Zhuravleva, postgraduate student at the Department of Physical, Colloid and Analytical Chemistry, Belarusian State Technological University (Minsk, Republic of Belarus).

https://orcid.org/0009-0009-2162-0202

ya.yu.zhuravleva@mail.ru

Vladimir M. Kononovich, Researcher of Physical and Chemical Investigations Method Center of Belarusian State Technological University (Minsk, Republic of Belarus).

https://orcid.org/0009–0003–9230–7025

rfarfa@mail.ru